Science and Technology for Energy Transition **79**, 11 (2024)

https://doi.org/10.2516/stet/2024006

Available online at:
stet-review.org

REGULAR ARTICLE OPEN ACCESS

Biodiesel production from hempseed (*Cannabis sativa* L.) oil: Providing optimum conditions by response surface methodology

Cemal Yazilitaş[1], Zeki Yilbaşi[1,*], and Murat Kadir Yeşilyurt[2]

[1] Department of Automotive Technology, Yozgat Bozok University, Yozgat 66200, Türkiye
[2] Department of Mechanical Engineering, Yozgat Bozok University, Yozgat 66200, Türkiye

Received: 9 September 2023 / Accepted: 23 January 2024

Abstract. This study focuses on the optimization of biodiesel synthesis using non-edible hempseed oil as the feedstock. The response surface method was used to find the best methanol: oil molar ratio, catalyst concentration, reaction temperature, and reaction duration for the transesterification process. The center composite design experimental design was used to make the design. A total of 30 cycles were conducted to adjust the four parameters at five different levels in order to optimize the biodiesel production process. It was found that the best conditions for transesterification of hempseed oil were a KOH catalyst concentration of 0.80 wt.%, a molar ratio of 7.41:1, a reaction time of 62.83 min, and a reaction temperature of 61.92 °C. Under these optimized reaction conditions, the predicted biodiesel yield was 95.57%, while the experimental yield was 95.24%. The biodiesel produced using the optimized parameters was analyzed for its properties, and the findings demonstrated that it met the requirements of EN 14214, a standard for biodiesel quality. The optimization of the biodiesel synthesis process using non-edible hempseed oil contributes to the exploration of alternative and sustainable feedstocks for biodiesel production. The values of the produced biodiesel within the standard range demonstrate its suitability for commercial applications and strengthen the potential of hemp seed oil as a suitable raw material for biodiesel production.

Keywords: Cannabis seed oil, Optimization, Response surface methodology, Fuel properties.

Nomenclature

Abbreviations

ANOVA	Analysis of Variance
AV	Acid Value
BR	Basic Runs
CCD	Central Composite Design
CH_3OH	Methanol
CI	Compression Ignition
CN	Cetane Number
DU	Degree of Unsaturation
FAME	Fatty Acid Methyl Ester
FFA	Free Fatty Acid
HHV	Higher Heating Value
HSO	Hemp Seed Oil
HSOME	Hempseed Oil Methyl Ester
KOH	Potassium Hydroxide
LCSF	Long Chain Saturated Factor
OS	Oxidation Stability
RSM	Response Surface Methodology

Symbols

A	Methanol-to-oil molar ratio
Adj. R^2	Adjusted R^2 value
B	Catalyst concentration
b	Blank volume
C	Reaction temperature
D	Reaction time
F-value	F-test value
n	Number of input factors
n_0	Number of repetitions
P-value	Probability value
Predicted R^2	Predicted R^2 value
R^2	Correlation coefficient
SS	Sum of Square

* Corresponding author: zeki.yilbasi@yobu.edu.tr

v	Volume of titer solution
w	Mass of the oil
X	Independent factor
Y	Yield

1 Introduction

Energy consumption and social development are closely linked, as energy is a key factor for human well-being and economic growth. However, not everyone has equal access to energy, and this creates significant disparities in the level of development among countries and regions. This article explores the relationship between energy consumption and social development, and how it affects the prospects of achieving sustainable development goals [1, 2]. It also examines the challenges and opportunities for increasing access to energy in developing countries, and how this can enhance their social and economic outcomes [3, 4].

The manufacturing industry depends heavily on energy, which is a key indicator of economic and social development potential. However, energy consumption also increases with the level of development and welfare, as well as with the growing demand for machines and transportation in a rapidly industrializing and urbanizing world. This poses significant challenges for energy efficiency, which is essential for using local resources optimally, ensuring resource diversity and security, enhancing productivity, and protecting the environment [5]. The global energy markets have faced unprecedented shocks and volatility since 2022, due to the war in Ukraine that erupted amid the ongoing COVID-19 pandemic. This has raised serious concerns about energy scarcity and security and has hindered global efforts to achieve universal access to sustainable, affordable, accessible, and reliable modern energy by 2030 [6, 7].

Today, most of the energy used is derived from sources other than fossil fuels like natural gas, coal, and oil, which account for approximately 13% of total energy consumption [8, 9]. Since the transportation sector is responsible for the largest proportion of the world's total energy consumption, oil has maintained its position as the most important energy source until today [10]. Furthermore, according to projection studies carried out by numerous international institutes and organizations, oil's position in the ranking of primary energy use will not change in the long term [11]. Internal combustion engines are a part of the growing automobile market, which is being fueled by the fast increase in the world's population, industrialization, and economy [12]. The expansion in the transportation industry, including private vehicle travel, public transportation, and freight, is also growing for the same reasons. Due to this, demand for oil-based energy has skyrocketed, particularly in industrialized and developing nations [13]. Data on daily global oil consumption indicate that the amount of oil consumed rises every year. Only by increasing daily world oil output will this increase be able to be satisfied [14]. Compression-ignition internal combustion engines, the majority of which use diesel fuel with a petroleum basis, are frequently used in the transportation sector. However, because of the chemical composition of diesel fuel, air pollution complaints resulting from emissions from combustion are growing daily and posing some risks [15]. Researchers are concentrating on the use of biodiesel fuels derived from various petroleum sources rather than conventional diesel in an attempt to address these issues [16].

The quick advancement of renewable energy sources and the efficient use of finite resources are crucial for the entire globe [17]. Fossil fuels are expected to be phased out in the not-too-distant future due to energy crises, rising oil prices, and air pollution as a result of emissions. Among renewable energy sources for compression ignition engines, biodiesel is a viable option with both technical and economic promise [5]. Long-chain fatty acid alkyl esters generated from vegetable oils, animal fats, or waste oils are what are referred to as biodiesel [18].

Around a quarter of a million different plant species are known to exist on Earth [19]. Although the oils of thousands of plants have been studied, only about 2% of them are commercially exploited. On the other hand, around twenty-two oil plants are produced commercially across the globe [20]. Nowadays, oil produced from canola, cotton, palm, soybean, and sunflower oils accounts for more than 90% of all oil production worldwide. Both internationally and domestically, oilseed crops are recognized as strategically important agricultural products. The world's traditional oilseed plants, such as soybean, canola, cotton, and sunflower, have expanded their cultivation regions over time [21]. However, the planting fields of hemp, poppy, and safflowers, which can replace traditional oilseed crops, have unfortunately not expanded compared to the past [22].

Hemp is a type of herbaceous plant, and its main uses are as an oilseed, a source of industrial-grade fiber, as well as for food, medicinal, and recreational purposes [23, 24]. According to reports, Western and Central Asia are the native homes of the annual crop known as hemp. In India's sub-Himalayan regions, hemp is also grown. It can be grown in barren lands [25]. Hemp has long been used as a feedstock in the textile industry, as is widely known [26]. Additionally, it was also noted that hemp has a wide range of uses, including the construction industry, automotive, plastics, high-quality absorbents, paper, agriculture, personal cleaning, and healthcare. However, the development of these plants has as its specific goals the extraction of drugs, crude oil, and fiber [27, 28]. Non-edible oil made from industrial-grade hempseeds has recently become quite important for nations. On the other hand, the aforementioned literature review revealed that a small number of studies were conducted to produce biodiesel from hempseed oil. The Free Fatty Acid (FFA) count of hempseed oil was detected to be less than 2%, which was highlighted when the physical and chemical properties were measured to evaluate the properties of hempseed oil biodiesel [29, 30]. Hempseed has been considered a potential feedstock for methyl ester synthesis thanks to its 26%–38% oil content. Additionally, its fiber contains a high concentration of minerals, 20%–30% carbs, 25%–35% protein, and 10%–15% insoluble fiber [25].

Vegetable oils have distinct chemical structures from petroleum-derived fuels, so their direct use as fuel in

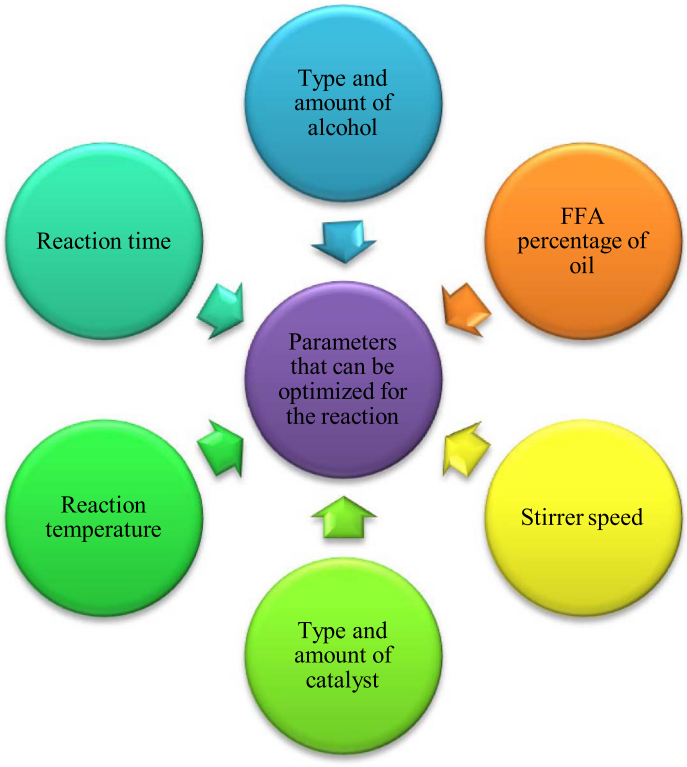

Figure 1. Parameters with the potential to impact the transesterification reaction.

Compression Ignition (CI) engines can lead to problems [31]. In order to ensure the use of vegetable oils as fuel, research is carried out on two main topics: changing engine settings and increasing the fuel efficiency of vegetable oils [32]. The viscosity of vegetable oils is the main focus of research on enhancing their fuel characteristics [33]. Thermal and chemical techniques are used to lower the viscosities of oils. In the thermal approach, the viscosity of the oil is reduced by raising its temperature through preheating. Dilution, pyrolysis, microemulsion, and transesterification are categories for chemical processes [34]. The most common one for biodiesel production is transesterification [35]. Fatty acid alkyl esters are formed when oils react with alcohol and catalysts in the course of the transesterification process [36]. The kind of alcohol and the alcohol to oil molar ratio, the type and concentration of the catalyst, the stirring rate, the amount of FFA, the reaction temperature, and the reaction time are the most crucial variables impacting the transesterification reaction [37].

The alkali-catalyzed transesterification technique has the drawback of being unsuitable for vegetable oils with high FFA content [38]. This is because problems with emulsification and separation emerge from FFAs' reaction with the catalyst to create soaps [39]. Additionally, excessive soap creation hinders subsequent purification procedures like glycerol separation and water washing and lowers biodiesel yield [40]. Although various criteria have been published, a constant value for the maximum allowable FFA content in vegetable oil for alkali-catalyzed transesterification could not be determined. Although there are studies indicating that vegetable oils with up to 5% FFA can be subjected to transesterification reaction using an alkali catalyst, many researchers have mentioned that FFA should be kept below 2% for alkali-catalyzed transesterification [41–43]. A pre-esterification technique, which uses a homogenous acid-catalyzed procedure before transesterification, can be utilized to get around the challenges associated with the transesterification of oils with high FFA [44].

Various pre-esterification and transesterification reaction factors, reaction temperature, and reaction time, including the amount of alcohol, the concentration and type of catalyst, and the FFA percentage of the oil, have an impact on the quality and yield of biodiesel. Figure 1 presents the variables that impact the transesterification reaction. In the stoichiometric transesterification reaction, 3 moles of methanol are required for every mole of triglyceride in order to create 3 moles of methyl esters and one mole of glycerol [41, 45]. Therefore, the ideal molar ratio of methanol to triglyceride is 3:1 [46]. To encourage the complete conversion of oils to Fatty Acid Methyl Ester (FAME), the alcohol-to-oil ratio employed in the reaction must be significantly greater than this and varies depending on the type of catalyst and the quality of the oil being used [47]. The conversion of triglycerides to fatty acid esters typically rises with an increment in catalyst concentration [48]. A lack of catalyst causes the conversion reaction to be incomplete and the amount of fatty acid esters to decrease, while an abundance of catalyst leads to soap formation, reducing the yield of the final product [49–51].

The transesterification reaction, which converts oil and alcohol into biodiesel and glycerol, can be performed at different temperatures depending on the amount and type of

the reactants [52]. The optimal reaction temperature should be close to the boiling point of the alcohols, which is usually around 64.7–78.3 °C for methanol and ethanol. If the reaction temperature exceeds the boiling point of the alcohol, the alcohol can vaporize and escape from the reaction mixture, reducing the biodiesel yield [53]. The reaction rate and conversion of oil to biodiesel depend on the initial stages of the transesterification process. It has been reported that the reaction is slow for the first five minutes, and then accelerates rapidly [54]. After 30 min, the conversion reaches about 80%, and after 60 min, there is no significant increase in the biodiesel yield [55].

Various optimization studies have been conducted to determine the optimal conditions for the synthesis of biodiesel from different feedstocks, such as vegetable oils, animal fats, and waste oils. Response Surface Methodology (RSM) is a widely used statistical technique for optimizing complex processes with multiple variables and responses. RSM has been used to improve the transesterification of many vegetable oils, including Jatropha curcas-Ceiba pentandra oil blend [56], papaya oil [47], flaxseed oil [57], yellow mustard oil [5], Terminalia bellerica [58], flaxseed oil [59], palm oil [60], sour cherry kernel oil [61], Azadirachta India-derived oil [62], soybean oil [63], Jatropha-algae oil [64] blend, and more. The main factors that affect biodiesel production from vegetable oils are the catalyst concentration, the methanol-to-oil ratio, the reaction time, and the reaction temperature. RSM can help find the optimal values of these factors that maximize biodiesel yield and quality.

Hemp Seed Oil (HSO) is a promising feedstock for biodiesel production, as it has a high oil content and a favorable fatty acid profile. However, the optimal conditions for the transesterification of HSO into biodiesel have not been determined yet. To the best of the authors' knowledge, hempseed oil has not yet had the transesterification reaction parameters optimized using RSM, despite being a promising feedstock for the generation of biodiesel. The major goal of this study was to optimize the reaction parameters for the production of high-yield biodiesel from Hemp Seed Oil (HSO) using RSM-based Central Composite Design (CCD). Following that, the EN 14214 biodiesel standard was used to evaluate and compare the fuel characteristics of the biodiesel generated under ideal circumstances.

2 Materials and methods

In this available work, optimization of transesterification reaction operating parameters was performed by applying an RSM approach involving CCD. Due to a lack of research, HSO was chosen and experimented with for this goal. Materials were procured according to their suitability, and necessary inspections were carried out. Additionally, a suitable and feasible methodology was proposed for the utilization of the acquired alternative fuel sample in subsequent research.

2.1 Materials

The simplicity and convenience of obtaining the reagents and other components needed in the biodiesel manufacturing stage and analysis led to their preference. This experimental work was carried out using analytical-grade chemicals. Without any additional purification, chemicals were utilized in their original state. Hempseeds were bought from a company specializing in oilseeds in Ankara, Turkey. Methanol (CH_3OH) and Potassium Hydroxide (KOH) were selected as lower-order alcohol and as base homogeneous catalysts, respectively, due to their reaction activities involved in the transesterification process. KOH pellets (≥90% purity) and methanol (≥99.9% purity) were provided by *Tekkim Chemical Company* (Turkey) and *Merck Chemical Company* (Darmstadt, Almanya), respectively. *S & H Labware* (Turkey) provided 125-mm filter paper. The *Norateks Chemical Company* (Istanbul, Turkey) supplied the phenolphthalein indicator, and the KOH solution (0.1 N) was utilized to calculate the acid value. Using the Millipore Direct-Q 8UV system, distilled water was acquired for the washing procedure. Other pieces of equipment used in the trials, such as spoons, glasses, magnetic stirrer bars, etc., were purchased from a local supplier of ISO 9001 Quality Management certificates and EN ISO 17025 certification.

2.2 Methods

2.2.1 Extraction of hempseed oil

Cannabis sativa L. seeds were purchased, sorted, and cleaned. To retain the oil's purity, the seeds were cold-pressed using the GM1500 brand shown in Figure 2. First of all, the dried seeds were crushed straight into it without using any pre-crushing techniques since the hemp seeds' size was appropriate for the oil extraction equipment. Firstly, the cold press machine's seed input unit was where the seeds were placed. The nozzle thermostat was adjusted to 120 °C to allow the oil to flow easily from the nozzle, which was then compressed using a screw press. Using a filtration device for purification, the oil passing through the mesh filter on the nozzle during pressing was exposed to filtering. 0.25 kg of HSO was yielded from 1 kg of hemp seeds.

In order to use gravity and the distinctness of density to help the pulp granules subside, the yielded HSO was placed in a sealed glass cup for a week. The samples' tops were dumped into a different cup. Then, using basic cloth materials, the filtering step was performed on this HSO to take out the suspended pulp components. In this way, an enhanced filtering process was carried out using qualitative filter paper. Hemp seed filtered clean oil, and waste cake (used as animal food) are illustrated in Figure 3.

2.2.2 The testing equipment required for producing HSOB

In this experimental study aiming to produce biodiesel fuel using HSO, a one-step transesterification procedure was used since the FFA content of the crude oil appeared to be acceptable. It is widely accepted that the FFA content should be lower than 2%, although some authors have suggested different considerations for determining the number of stages required in the transesterification process when utilizing a homogeneous base catalyst [42, 65, 66]. An

Figure 2. HSO production from hemp seeds by the cold-press method.

Fig. 3. Illustration (a) Hemp seed, (b) filtered HSO, and (c) oil cake.

acid-base titration procedure is used to determine the FFA content of the HSO favored for this investigation. A single-stage transesterification reaction was preferred, as the FFA content of HSO was determined to be 0.98%.

A small-scale laboratory-style biodiesel batch reactor was developed in order to achieve this goal. The biodiesel reactor mentioned above is made up of a condensation system, a hot plate magnetic stirrer, a 250-mL flat-bottomed, three-necked flask that is connected to a reflux condenser to prevent the used alcohol from vaporizing during the reaction, a sampling inlet, and an outlet.

2.2.3 The method used to produce biodiesel from HSO

The major processing conditions that affect the yield of transformation and have been recognized by many studies include the methanol/oil molar ratio, amount of catalyst, reaction temperature, and reaction time [67–71]. The methanol's boiling point restricted the reaction temperature. Based on the available literature, the characteristics of the oil, and the outcomes of our prior studies, the ranges of the selected variables were established. The aforementioned variables were taken into account for the transesterification process optimization in the current study to create *Cannabis sativa* L. seed oil biodiesel with the highest percentage of yield.

As an overview, the single-stage transesterification procedure is as follows: The three-necked flat-bottom batch reactor was first filled with 100 g of *Cannabis sativa* L. seed oil, and the temperature was raised to the necessary level. The stirrer speed was fixed at 800 rpm for all experiments. The remeasured quantity of base catalyst (KOH) was dissolved in the necessary concentration of alcohol to create the methanol-catalyst combination. The produced methoxide solution was gradually added to the reactor with the use of a funnel after the temperature of the *Cannabis sativa* L. seed oil reached the appropriate level. Following the pouring process, the reaction time was started, and this time

was monitored with a stopwatch. At the conclusion of the reaction's allotted time, the mixture in the reactor was emptied into a 250-mL separating conical funnel. Following the 8-hour settling time, the glycerol precipitated on the bottom layer was removed from the separatory funnel using a drain valve. The crude biodiesel was then spilled into a glass beaker, and it was heated to 75 °C to eliminate excess methanol from the biodiesel. The temperature was lowered to 55 °C before the washing process started. The temperature was constant to prevent either sudden cooling of the crude biodiesel or sudden heating of the distilled water. To remove unreacted catalysts, soap, and other impurities, the product was washed with 20% of the volume of distilled water at the same temperature. With the aid of the valve, the wastewater was withdrawn from the funnel, and the cleaned biodiesel was heated until it reached 120 °C to begin the dewatering process. Finally, the biodiesel was kept in a glass cup in a dark place to rest and reduce the temperature. The samples were measured using a precision scale after they reached room temperature.

For a better understanding of HSOB production from HSO utilizing the transesterification reaction, the flow chart is shown in Figure 4.

After the methyl ester synthesis from HSO was accomplished at the optimal study conditions, taking into account the analytical findings of the RSM's approach, several of the significant physicochemical characteristics were investigated in accordance with the EN test method. In order to draw a conclusion, the results were contrasted with the EN 14214 international biodiesel standards.

2.2.4 Experimental design and statistical analysis

RSM was used in the optimization process to examine the effects of the methanol-to-oil molar ratio (A), catalyst concentration (B), reaction temperature (C), and reaction time (D) on biodiesel production from HSO. Table 1 shows the levels selected for these parameters. In the selection of the factor levels of the variables investigated, the variables of the biodiesel production process, the estimated operating limits within which the biodiesel yield can be maximized, and variables that affect preliminary tests were taken into account. The boiling point of methanol restricted the maximum reaction temperature to 70 °C. The ranges of the chosen variables were established utilizing the outcomes of our prior studies and oil characteristics.

The equation below is used to obtain the biodiesel yield percentage [57]:

$$\text{The biodiesel yield (\%)}: \; Y = \frac{\text{produced biodiesel (g)}}{\text{used oil in the reaction (g)}} \times 100. \quad (1)$$

Equation (2) is used to calculate the total number of experimental runs in a CCD model.

$$\text{BR} = 2^n + (2 \times n) + n_0 \quad (2)$$

where BR (Basic Runs) is the number of experimental runs, n (4) is the number of input factors, and n_0 (6) is the number of repetitions [72].

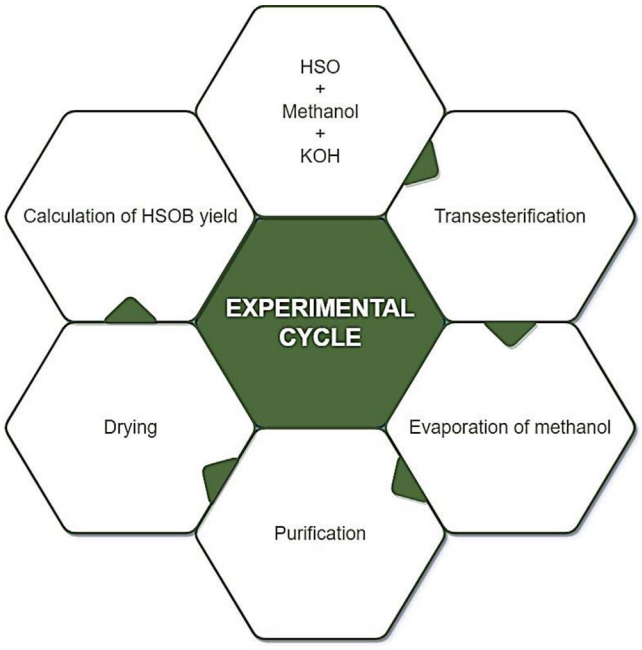

Figure 4. The cycle used in the experiment to obtain HSOB and determine the yield.

The CCD, which incorporates 4 independent variables at 5 levels, was used to carry out this investigation. Design summary of the CCD: 30 basic runs, 2 basic blocks, 4 continuous factors, 1 replicate, and full factorial (two-level factorial). Point types of the CCD: 2 center points in the axial, 4 center points in the cube, 8 axial points, and 16 cube points. The results are shown in Table 3 as responses (yields).

To develop a mathematical model, the experimental data were analyzed with RSM using Minitab 21.3.1 software. A quadratic polynomial equation is used to relate the response to the factors [73].

$$Y = b_0 + \sum_{i=1}^{k} b_i X_i + \sum_{i=1}^{k} b_{ii} X_i^2 + \sum_{i_{i>j}}^{k} \cdot \sum_{j}^{k} b_{ij} X_i X_j + e \quad (3)$$

where Y is the response (the yield), X_i and X_j are independent factors, b_0 is the offset term, b_i, b_{ii}, and b_{ij} are coefficients of regression, k is the number of factors investigated, i is the linear coefficient, j is the quadratic coefficient and e is the random error.

2.2.5 Characterizations and the fatty acid composition of fuel

The fatty acid profile of HSOB was analyzed using a Shimadzu QP2010 model Gas Chromatograph (GC). In accordance with EN and ASTM standards, the basic physical and chemical properties of HSOB and some fuel properties have been determined. Density (EN ISO 3675), pH, copper strip corrosion (EN ISO 2160), flash point (ASTM D93), cloud point (ASTM D2500), linolenic acid methyl ester (EN 14103), freezing point, pour point (ASTM D97), ash

Table 1. The variables and their corresponding levels for CCD.

Variables	Symbol	Levels				
		$-\alpha$	-1	0	1	α
Methanol to oil molar ratio (mol/mol)	A	2:1	4:1	6:1	8:1	10:1
Catalyst concentration (wt.%)	B	0.4	0.6	0.8	1.0	1.2
Reaction temperature (°C)	C	50	55	60	65	70
Reaction time (min)	D	20	40	60	80	100

content (EN ISO 3987), Group I metals (Na + K) and Group II metals (Ca + Mg) (EN 14538), and polyunsaturated (≥4 double bonds) methyl esters (EN 15779) determined in accordance with the specified standards. Calculations were made to determine the higher heating value, oxidation stability, iodine value, saponification number, cetane number, and kinematic viscosity (Table 2).

3 Results and discussion

The goal of this study is to maximize biodiesel yield by applying the RSM approach to optimize some crucial transesterification process variables. Equation (4) provides the quadratic polynomial model for the factors influencing biodiesel production. The experimental strategy established to produce biodiesel is shown in Table 3. Each of the thirty experiments was performed in triplicate, and the averages of the replicates were presented in Table 3.

$$Y = -92.0 + 7.57 \cdot A + 2.9 \cdot B + 4.411 \cdot C + 0.688 \cdot D - 0.2731 \cdot A^2 - 23.03 \cdot B^2 - 0.03580 \cdot C^2 - 0.002791 \cdot D^2 - 0.887 \cdot A \cdot B - 0.0289 \cdot A \cdot C - 0.01616 \cdot A \cdot D + 0.616 \cdot B \cdot C + 0.0428 \cdot B \cdot D - 0.00407 \cdot C \cdot D. \quad (4)$$

Examining the data presented in Table 4, A, C, D, A^2, B^2, C^2, D^2, $A{\cdot}D$, $B{\cdot}C$ and $C{\cdot}D$ gave P values less than 0.05. Thus, it significantly affected the yield of biodiesel produced from HSO. The B, $A{\cdot}B$, $A{\cdot}C$ and $B{\cdot}D$ values in the same table presented P values greater than 0.05. As a result, the yield of biodiesel produced from HSO was insignificantly affected. The final equation for equation (4) from the point of coded factors was produced after the not-significant parameters were removed, and it is shown below:

$$Y = 94.695 + 3.518 \cdot A + 0.12 \cdot B + 1.903 \cdot C + 1.855 \cdot D - 4.37 \cdot A^2 - 3.685 \cdot B^2 - 3.58 \cdot C^2 - 4.465 \cdot D^2 - 1.42 \cdot A \cdot B - 1.155 \cdot A \cdot C - 2.585 \cdot A \cdot D + 2.465 \cdot B \cdot C + 0.685 \cdot B \cdot D - 1.63 \cdot C \cdot D. \quad (5)$$

The final equation, expressed with regard to actual factors, is found in equation (6).

$$Y = -92.0 + 7.57 \cdot A + 4.411 \cdot C + 0.688 \cdot D - 0.2731 \cdot A^2 - 23.03 \cdot B^2 - 0.03580 \cdot C^2 - 0.002791 \cdot D^2 - 0.01616 \cdot A \cdot D + 0.616 \cdot B \cdot C - 0.00407 \cdot C \cdot D. \quad (6)$$

Each input factor's percentage contribution and associated P-values are disclosed using the Analysis of Variance (ANOVA). The outcomes of the ANOVA were displayed in Table 4. In this investigation, a significance level of 0.05 was used to determine if a result was significant or insignificant. Accordingly, the effects of these parameters on biodiesel production are significant when the P value is less than 0.05 and inconsequential when the P value is more than 0.05. The developed model was detected to be significant at a 95% confidence level, taking into account the calculated F value of 26.72 with a very low probability value. Thanks to this high significance, it turns out that the model applied to predict the yield of HSOB is also highly reliable.

The residual error was determined to be 2.14 in the "lack of fit test," which compared the residual error to the pure error. It suggests that, in comparison to pure error, lack of fit is not significant. The P-value of the lack of fit calculated as 0.207 (insignificant) is considered good for model fit. The coefficient of determination (R^2) to check the appropriateness of the mathematical model was used. Calculated values for R^2, adjusted R^2, and forecasted R^2 were 0.9614, 0.9255, and 0.8094, respectively. It can be determined from these values how well the assembly-fitting model performs. The model must also pass the Coefficient of Variation (C.V.) test, which requires a C.V. of less than 10%. The C.V. value of 0.76% indicates its suitability for the predicted biodiesel yield from HSO.

The actual yield of HSOB produced and the predicted results by RSM for biodiesel yield are shown in Figure 5. The experimental data and predicted value are represented by the horizontal (x) and vertical (y) axes, respectively. Also, the line in Figure 5 indicates a perfect fit. Moreover, it can be observed from Figure 6 that the ANOVA results are reliable for this investigation as the experimental values show normality.

The plots of residuals were examined to evaluate the model's correctness. The differences between the response's actual and predicted values (the biodiesel yield) are known as residuals. A straight line corresponding to the normal residual plot represented a successful fit, as seen in the normal possibility graph in Figure 6a. In the *versus* fits graph in Figure 6b, the agreement between the predicted

Table 2. The equations used to predict fuel properties [74–77].

Property	Formula	Definitions
Acid Value	$\mathrm{AV} = \frac{(v-b)\cdot 0,1\cdot 56.1}{w}$	AV: The acid value, v: The volume of the titer solution, b: The blank volume, w: The mass of the oil.
Free Fatty Acid	$\mathrm{FFA} = \frac{(v-b)\cdot 0,1\cdot 28.2}{w}$	FFA: Free Fatty Acid.
Molecular Weight	$\mathrm{MW} = 3{\cdot}\mathrm{AMW_{FA}} + \mathrm{WGB}$	$\mathrm{AMW_{FA}}$: The Average Molecular Weight of all Fatty Acids, WGB: Weight of Glycerol Backbone.
Saponification Number	$\mathrm{SN} = \sum\left(\frac{560\cdot A_i}{\mathrm{MW}_i}\right)$	SN: Saponification Number, A_i: The percentage of each component in the FAME.
Iodine Value	$\mathrm{IV} = \sum\left(\frac{254\cdot C_{\mathrm{DB}}\cdot A_i}{\mathrm{MW}_i}\right)$	IV: Iodine Value, C_{DB}: The number of double bonds of each FAME.
Cetane Number	$\mathrm{CN} = 46.3 + \frac{5458}{\mathrm{SN}} - 0.225\cdot \mathrm{IV}$	CN: The Cetane Number of FAME.
Higher Heating Value	$\mathrm{HHV} = 49.43 - [0.041{\cdot}\mathrm{SV} + 0.015{\cdot}\mathrm{IV}]$	HHV: The Higher Heating Value of FAME.
Cloud Point	$\mathrm{CP} = 0.526{\cdot}(C16{:}0) - 4.992$	CP: The Cloud Point of FAME.
Long Chain Saturated Factor	$\mathrm{LCSF} = 0.1{\cdot}(C16{:}0) + 0.5{\cdot}(C18{:}0) + (C20{:}0) + 1.5{\cdot}(C22{:}0) + 2{\cdot}(C24{:}0)$	LCSF: The Long Chain Saturated Factor of FAME.
Cold Filter Plugging Point	$\mathrm{CFPP} = 3.1417{\cdot}\mathrm{LCSF} - 16.477$	CFPP: The Cold Filter Plugging Point.
Density	$D = 0.8463 + \frac{4.9}{\mathrm{MW}_i} + 0.0118\cdot C_{\mathrm{DB}}$	D: The density of FAME.
Degree of Unsaturation	$\mathrm{DU} = \sum(\mathrm{MUFA}{:}1,\%) + 2\cdot\sum(\mathrm{PUFA}{:}2,3,4,\%)$	DU: The degree of unsaturation parameter, MUFA: monounsaturated fatty acids, PUFA: polyunsaturated fatty acids.
Oxidation Stability	$\mathrm{OS} = \frac{[(C16{:}1 + C18{:}1 + C20{:}1 + C22{:}1) + (10,3\cdot C18{:}2) + (21,6\cdot C18{:}3)]}{100}$	OS: The Oxidation Stability of FAME.
Kinematic viscosity	$\ln(\eta_i) = -12.503 + [2.496{\cdot}\ln(\mathrm{MW}_i)] - (0.178{\cdot}N_s)$	$\ln(\eta_i)$: The kinematic viscosity of FAME, N_s: The number of double bonds in the monounsaturated and polyunsaturated fatty acids.
Pour Point	$\mathrm{PP} = 0.571{\cdot}C16{:}0 - 12.24$	PP: The Pour Point of FAME.

and actual biodiesel values according to the proximity or distance of the predicted biodiesel yield to the 0-residual line is displayed. The histogram in Figure 6c gives an idea about the validity and accuracy of the model. It is understood that the three peaks (modes) with the highest frequency of about 4.8 are the regions where the residual values are concentrated at −0.75, 0.25, and 0.50, respectively. This is more clearly noticeable when looking at the residual values corresponding to the observation order in the *versus* order graph in Figure 6d.

Figure 7 presents the Pareto plot of the standardized effects on biodiesel yield. A significance level threshold value is displayed on the Pareto chart. For the effect to be significant, the standardized effects of the parameters must be greater than the threshold value. In this graph, the bars representing the factors A, DD, AA, BB, CC, C, D, AD, BC, and CD cross the baseline with a standardized effect value of 2.13. It can be concluded that all factors except factors AB, AC, BD, and B have a significant effect on biodiesel yield.

Figure 8 shows the contour plots for the yield of HSOB as a function of A and B, A and C, A and D, B and C, B and D, and C and D, respectively, under optimum conditions.

Table 3. Design of the experiment to produce biodiesel from HSO.

Run	A	B	C	D	Methanol to oil molar ratio (mol/mol)	Catalyst concentration (wt.%)	Reaction temperature (°C)	Reaction time (min)	Produced biodiesel (wt.%)	Predicted biodiesel (wt.%)	Residual (wt.%)
1	−1	−1	−1	−1	4:1	0.6	55	40	85.73	86.05	−0.3228
2	1	−1	−1	−1	8:1	0.6	55	40	92.68	92.15	0.5284
3	−1	1	−1	−1	4:1	1.0	55	40	84.88	85.29	−0.4112
4	1	1	−1	−1	8:1	1.0	55	40	90.84	89.97	0.8692
5	−1	−1	1	−1	4:1	0.6	65	40	88.26	88.11	0.1452
6	1	−1	1	−1	8:1	0.6	65	40	93.18	93.06	0.1224
7	−1	1	1	−1	4:1	1.0	65	40	90.71	89.82	0.8928
8	1	1	1	−1	8:1	1.0	65	40	93.29	93.34	−0.0508
9	−1	−1	−1	1	4:1	0.6	55	80	89.57	89.66	−0.0936
10	1	−1	−1	1	8:1	0.6	55	80	92.40	93.18	−0.7768
11	−1	1	−1	1	4:1	1.0	55	80	89.58	89.59	−0.0068
12	1	1	−1	1	8:1	1.0	55	80	91.39	91.68	−0.2908
13	−1	−1	1	1	4:1	0.6	65	80	89.34	90.10	−0.7576
14	1	−1	1	1	8:1	0.6	65	80	92.72	92.45	0.2652
15	−1	1	1	1	4:1	1.0	65	80	91.81	92.48	−0.6748
16	1	1	1	1	8:1	1.0	65	80	93.86	93.42	0.4372
17	0	0	0	0	6:1	0.8	60	60	95.15	94.67	0.4772
18	0	0	0	0	6:1	0.8	60	60	94.11	94.67	−0.5628
19	0	0	0	0	6:1	0.8	60	60	93.83	94.67	−0.8428
20	0	0	0	0	6:1	0.8	60	60	95.01	94.67	0.3372
21	$-a$	0	0	0	2:1	0.8	60	60	87.45	86.78	0.6652
22	a	0	0	0	10:1	0.8	60	60	93.32	93.82	−0.5016
23	0	$-a$	0	0	6:1	0.4	60	60	91.33	90.88	0.4452
24	0	a	0	0	6:1	1.2	60	60	90.81	91.09	−0.2812
25	0	0	$-a$	0	6:1	0.8	50	60	89.49	89.19	0.2992
26	0	0	a	0	6:1	0.8	70	60	92.86	92.99	−0.1348
27	0	0	0	$-a$	6:1	0.8	60	20	87.50	88.36	−0.8608
28	0	0	0	a	6:1	0.8	60	100	93.08	92.05	1.0264
29	0	0	0	0	6:1	0.8	60	60	95.00	94.67	0.3272
30	0	0	0	0	6:1	0.8	60	60	95.07	94.67	0.3972

As anticipated, Figure 8 demonstrates a positive correlation between the molar ratio of methanol to oil and the yield of biodiesel. The molar ratio of methanol to oil is a crucial factor that significantly influences the biodiesel yield. The transesterification process is unable to reach completion when a limited amount of alcohol is used. However, it should be noted that the biodiesel yield does not exhibit a significant rise above the optimum methanol-to-oil ratio. It is important to note, however, that adding larger volumes of alcohol can increase the cost of the alcohol recovery process. An additional challenge is the difficulty of separating glycerol from biodiesel when larger quantities of methanol are used.

Figure 8 demonstrates a negative correlation between the concentration of catalyst utilized in the process and the yield of biodiesel. The observation of soap generation during the washing process is due to the overuse of catalysts. Furthermore, insufficient KOH prevents the reaction from being completed.

As seen in Figure 8, there is a positive correlation between the reaction rate and the duration of the reaction. During the first stages, the reaction exhibits a sluggish rate. Over time, the pace of the reaction gradually intensifies, leading to a corresponding increase in the yield of biodiesel.

The regression equation was solved to estimate the optimum reaction conditions for four parameters affecting the transesterification process, and the optimum conditions are presented in Figure 9. The optimum parameters were determined as follows: The molar ratio of methanol to oil (A) was found to be 7.4141:1, the catalyst concentration (B) was determined to be 0.8040 wt.%, the reaction temperature (C) was measured at 61.9192 °C, and the reaction duration (D) was recorded as 62.8283 min. Under the

Table 4. ANOVA results of quadratic RSM.

Source	Degrees of freedom	Sum of squares	Mean squares	*F*-value	*P*-value	Degree of significance
Model	14	214.991	15.3565	26.72	0.000	Significant
Linear	4	116.741	29.1852	50.78	0.000	
A	1	74.272	74.2720	129.23	0.000	
B	1	0.086	0.0864	0.15	0.704	
C	1	21.736	21.7361	37.82	0.000	
D	1	20.646	20.6461	35.92	0.000	
Square	4	79.015	19.7539	34.37	0.000	
A^2	1	32.738	32.7375	56.96	0.000	
B^2	1	23.279	23.2787	40.50	0.000	
C^2	1	21.971	21.9710	38.23	0.000	
D^2	1	34.176	34.1764	59.46	0.000	
2-way interaction	6	19.235	3.2058	5.58	0.003	
$A \cdot B$	1	2.016	2.0164	3.51	0.081	
$A \cdot C$	1	1.334	1.3340	2.32	0.148	
$A \cdot D$	1	6.682	6.6822	11.63	0.004	
$B \cdot C$	1	6.076	6.0762	10.57	0.005	
$B \cdot D$	1	0.469	0.4692	0.82	0.381	
$C \cdot D$	1	2.657	2.6569	4.62	0.048	
Error	15	8.621	0.5747			
Lack-of-fit	10	6.991	0.6991	2.14	0.207	Not significant
Pure error	5	1.630	0.3261			
Total	29	223.612				
C.V. = 0.76%						
R^2 = 0.9614						
Adj. R^2 = 0.9255						
Predicted R^2 = 0.8094						

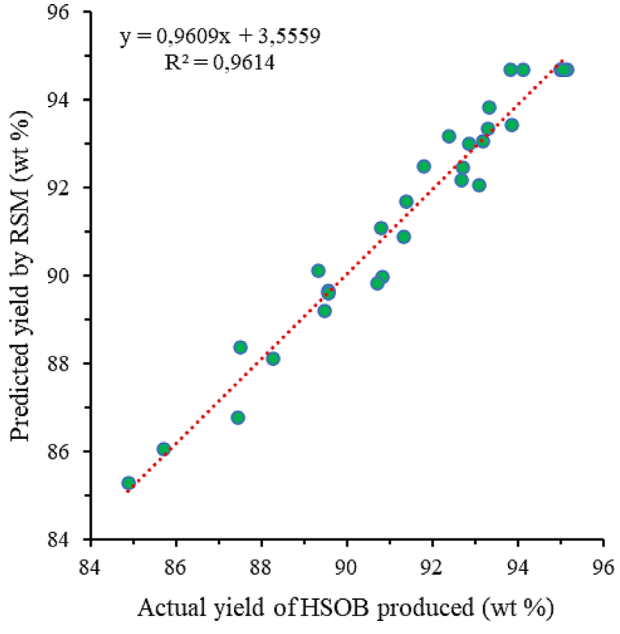

Figure 5. Actual yield *vs.* predicted yield.

circumstances that were determined to be optimal, the model predicted a biodiesel yield of 95.579%. Additionally, the experimental investigations were conducted using a small-scale biodiesel reactor to verify the accuracy and reliability of the proposed model. Consequently, the biodiesel yields for experiments 1, 2, and 3 were determined to be 95.13%, 95.25%, and 95.34%, respectively. The mean percentage of the three separate replicates was determined to be 95.24%, closely aligning with the theoretically expected rate. The difference between the actual and predicted values is quite minor. This phenomenon may be elucidated by considering the impact of unsung factors. Furthermore, the residual between the experimental and predicted values was calculated to be even less than 0.5%. Hence, there was a perfect match between the experimental and predicted values. The results indicate a significant level of similarity between the predicted and actual values.

The primary obstacles to achieving an integrated process are substantial capital expenditure on equipment, significant energy usage, and elevated manufacturing costs [76]. Table 5 presents the ranges of reaction parameters used and the maximum biodiesel yield attained in previous studies using several transesterification processes of new or

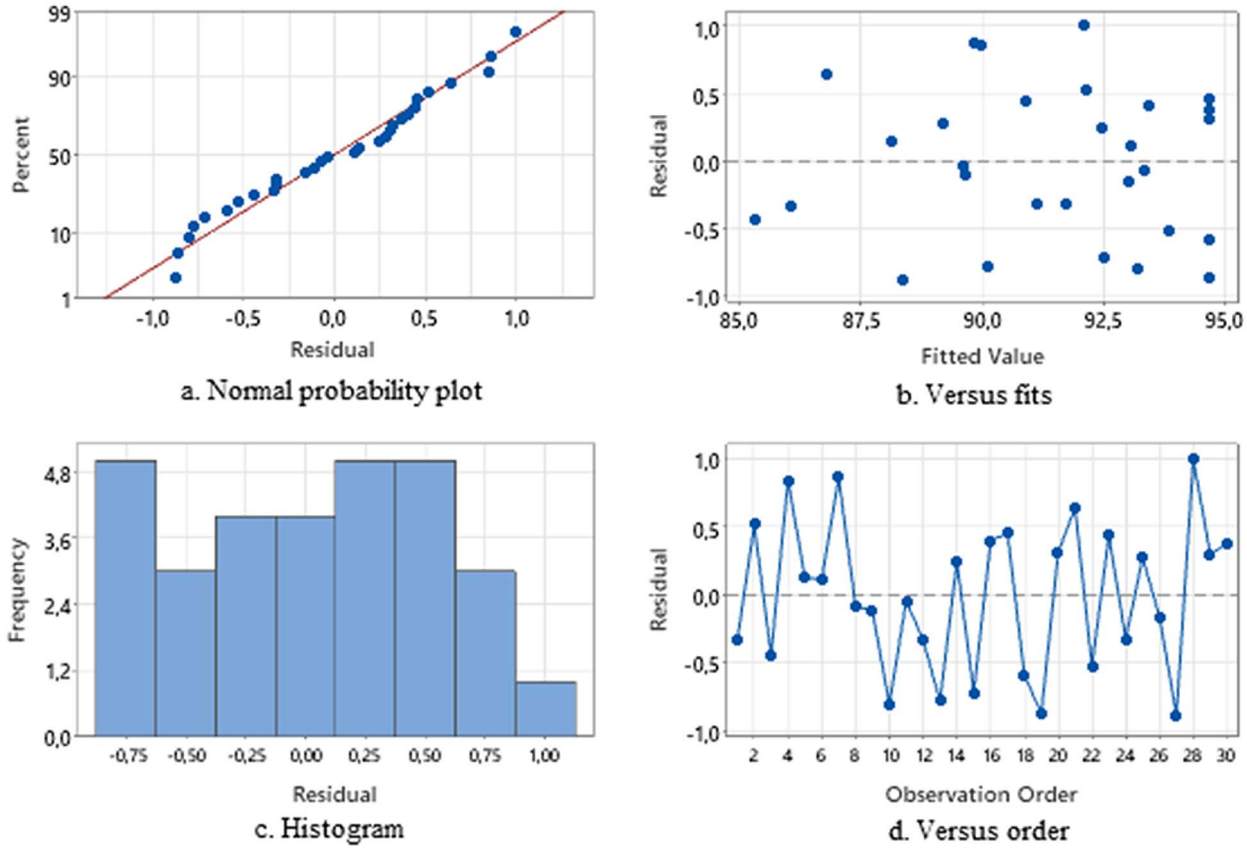

Figure 6. Residual plots for biodiesel yield.

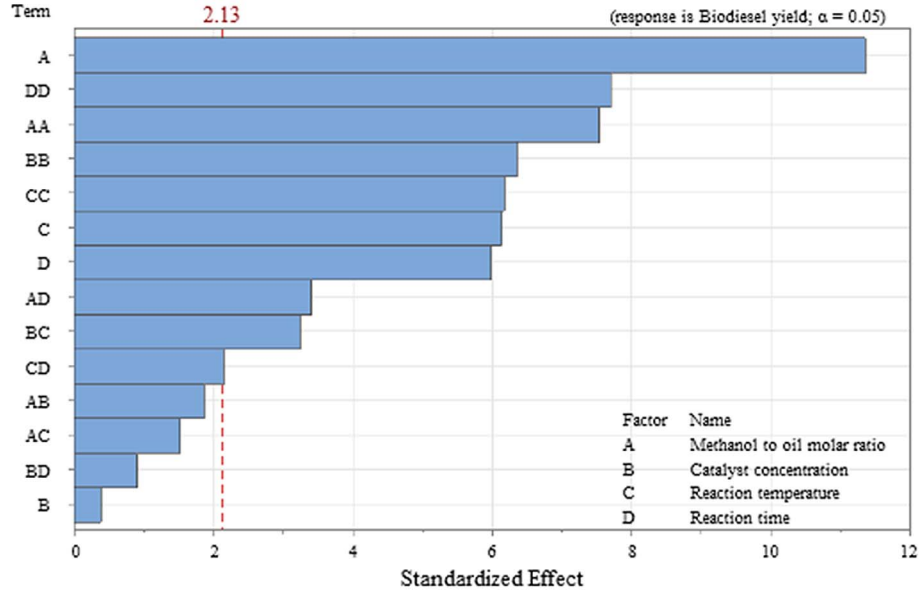

Figure 7. Standardized effects Pareto chart.

lesser-known oilseed or biodiesel raw materials, employing diverse optimization strategies. The maximal biodiesel yield from the current investigation as well as the reaction parameters are offered for comparison. It is important to acknowledge that there is not much research on the use of innovative feedstocks to optimize the transesterification process parameters. There is a need for further research by researchers to overcome this deficiency.

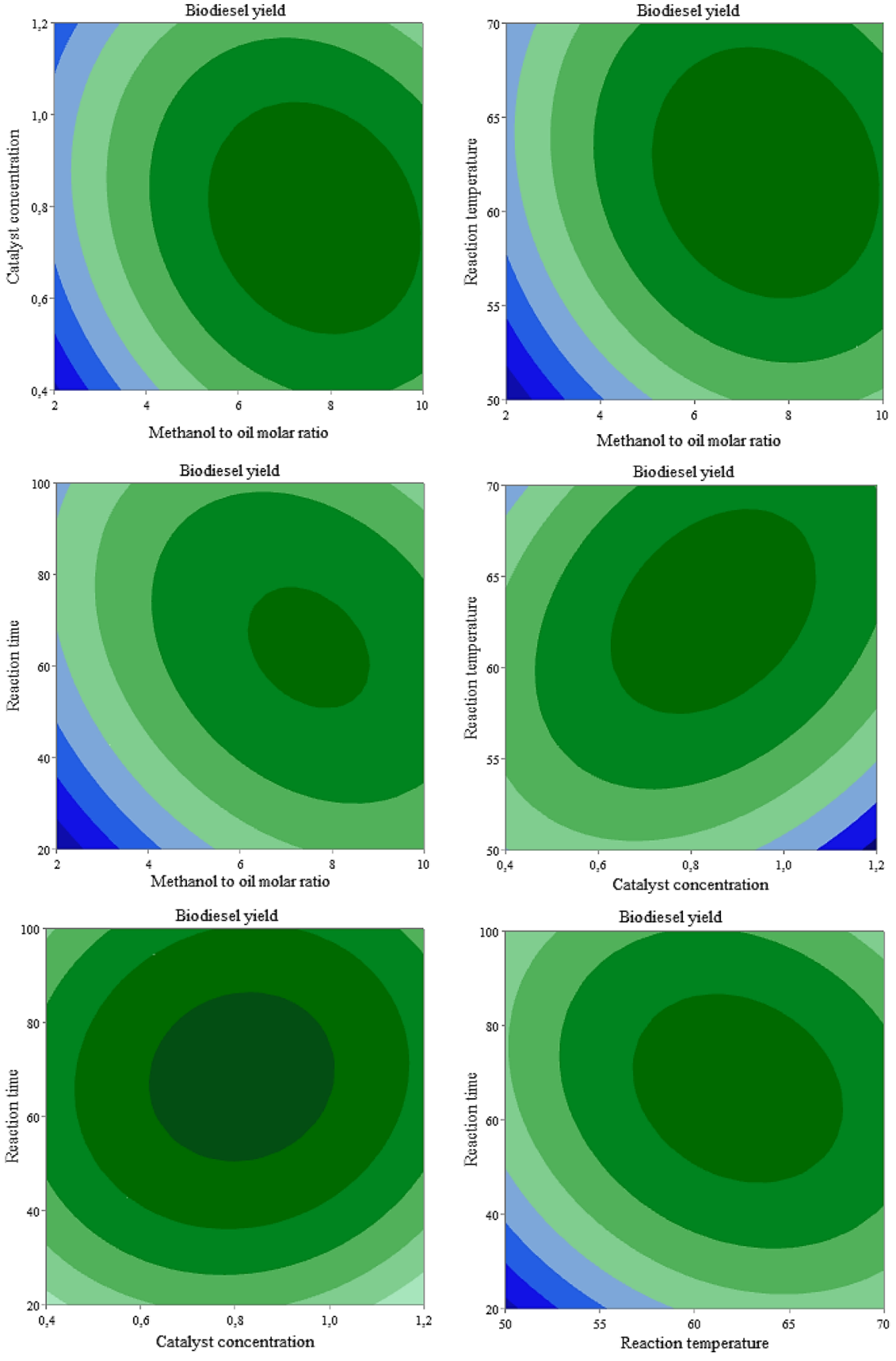

Figure 8. Contour plots of conversion to HSOB.

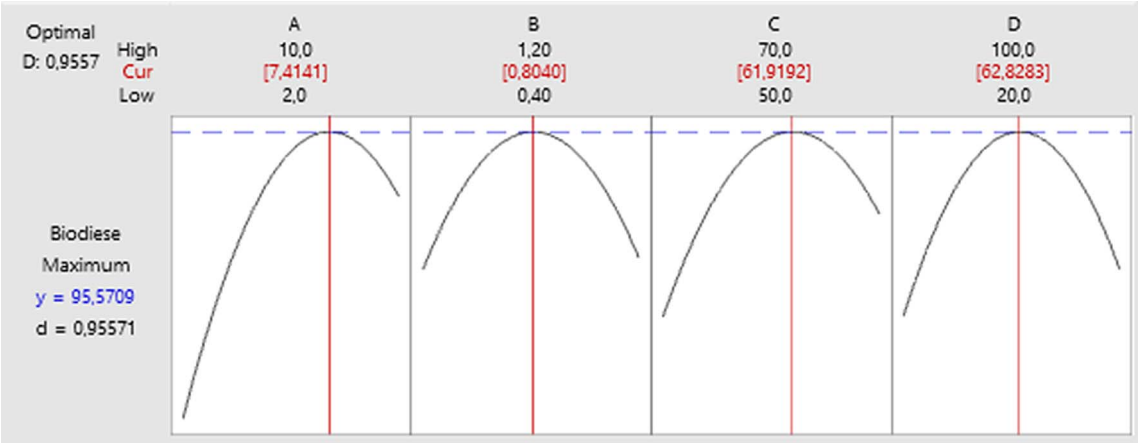

Figure 9. Optimum conditions.

The depiction of biodiesel is significant during the process of biodiesel conversion, as it determines its suitability as a feedstock for engine use. Typically, both edible and non-edible biodiesel varieties consist of saturated (SFA), monounsaturated (MUFA), and PolyUnsaturated Fatty Acids (PUFA). The fatty acid composition was determined by the use of Gas Chromatography (GC), as seen in Figure 10 for HSOB. Additionally, the results were organized and presented in a classified manner in Table 6. The composition of HSOB is characterized by a maximum linoleic acid content of 54.27%. Additionally, it includes 16.51% alpha-linolenic acid, 15.65% oleic acid, 7.01% palmitic acid, 3.22% stearic acid, and other acids with values less than 1%. This composition demonstrates a well-balanced proportion of saturated and unsaturated fatty acids. In addition, 17.13% MUFA content is indicative of quality biodiesel in terms of cold flow, oxidation stability, and improved combustion properties. Figure 10 and Table 6 illustrate the optimal balance of saturated and unsaturated fatty acids, resulting in enhanced ignition properties and improved oxidation stability. The total amount of MUFA and PUFA in HSOB, however, is relatively higher at 88.60%. This is positive for good flow properties and auto-oxidation, but negative for kinematic viscosity and acid value [82]. The proportion of unsaturated and saturated components in biodiesel plays a crucial role in determining its overall quality. The presence of unsaturated compounds enhances the fuel's capacity to perform well at low temperatures, while the saturation of the compounds contributes to the maintenance of oxidative stability and a high cetane number [83].

The fuel properties of biodiesel in accordance with EN standards are shown in Table 7. The quality of biodiesel is contingent upon fuel qualities, namely kinematic viscosity, density, etc. These essential variables are crucial for evaluating the fuel's suitability for use in diesel engines. Density is a notable attribute that has a direct influence on the efficiency of fuel injection in engines as well as on orifices, injector nozzles, and fluid flow inside pipelines [81]. The density of the HempSeed Oil Methyl Ester (HSOME) is 0.876 g/m^3, which is within the range of the EN 14214 standard. The density of HSOME is lower than the density of each biodiesel in Table 7.

Kinematic viscosity is another crucial aspect of biodiesel. Viscosity has an impact on the fluidity of biodiesel and is crucial for combustion, soot formation, and the formation of deposits. In the event of excessive viscosity, the occurrence of full combustion is impeded. Moreover, the elevated viscosity levels of the fuels might lead to the accumulation of carbon in various components, insufficient spraying, and a deterioration in atomization quality [5]. According to the study's findings, the HSOME has a viscosity of 4.329 mm^2/s, which is in accordance with the specifications of the EN 14214 standard.

The Cloud Point (CP) of a fuel is another important characteristic of it. This property refers to the temperature at which the presence of wax in diesel or bio-wax in biodiesel results in visible cloudiness. It is important to note that at this particular temperature, the fuel retains its fluidity and remains suitable for usage. For low-temperature runs, the CP is a crucial fuel property, and lower CP values are preferred. According to Table 7, all CP values differ substantially from each other. Since the EN 14214 standard is not known for the −1.3 °C CP value determined in this study, the ASTM D6751 (−3 °C to 12 °C) standard was checked, and it was determined that it complied. The biodiesel fuel's Pour Point (PP) is still another crucial aspect. The PP refers to the minimum temperature at which the flowability of an oil is observed. The temperature at which the PP occurs is lower in comparison to the temperature at which the CP occurs. Given that the PP value of −6.87 °C, as obtained in this research, is not recognized under the EN 14214 standard, an assessment was conducted to ascertain its compliance with the ASTM D6751 (−15 °C to 10 °C) standard. It was concluded that the PP value indeed adheres to the aforementioned standard.

Another factor that significantly affects combustion is the Flash Point (FP), which is the lowest temperature at which fuel vapor begins to burn. Fuels with a high FP pose less fire danger. The FP of HSOME is >120 °C, which satisfies EN 14214, as shown in Table 7. High FP is one of the advantages of biodiesel over petroleum-based fuel.

Table 5. The comparison of biodiesel production process parameters from *Cannabis sativa* L. seed oil with other feedstocks.

Feedstock	Biodiesel production equipment	Production process parameters							Optimization method	Optimum reaction conditions				Yield (%)	Refs.
		Catalyst		Alcohol		Reaction time (min)	Reaction temperature (°C)	Agitation intensity (rpm)		Catalyst amount (w/w)	Alcohol to oil molar ratio	Reaction time (min)	Reaction temperature (°C)		
		Type	Amount (w/w)	Type	Alcohol to oil molar ratio										
Cannabis sativa L. seed	Three-necked flat bottom flask, magnetic stirrer	KOH	0.4–1.2	Methanol	2:1–10:1	20–100	50–70	800	RSM, CCD	0.804	7.4141	62.8283	61.9192	95.24	This work
Jatropha-algae oil blend	A spherical glass reactor with a mechanical stirrer and a thermometer	KOH	0–2	Methanol	6:1–12:1	60–180	35–55	Absent	RSM, Box-Behnken	0.3	10	172	53	96	[64]
Grape seed	The flat-bottomed Erlenmeyer flask, magnetic stirrer	NaOH	0.143–1.657	Methanol	0.11545–0.3845	30–90	60	450	RSM, CCD	1.045	0.2758	66.6	60	97.7	[78]
Sterculia foetida	A round-necked flat bottom flask, magnetic stirrer	NaOH	0.55–1.55	Methanol	10–30 (v/v)	15–195	50–70	800	RSM, CCD	1.09	26% (v/v)	135	63	94.941	[79]
Orange peel	Three-necked flat bottom flask, magnetic stirrer	KOH	0.25–1	Methanol	3:1–9:1	30–90	45–65	350	RSM	0.67	6.27	58.16	53	97.21	[80]
Kusum	A around bottled flask fitted reflux type condenser, magnetic stirrer,	KOH	0–2	Methanol	0–12:1	30–150	50–70	500	RSM, CCRD	0.95	7.5	115	63.3	98.48	[68]
Sinapis alba L.	Three-necked flat bottom flask, magnetic stirrer	NaOH	0.2–1.0	Methanol	2:1–10:1	30–90	50–70	800	RSM, CCD	0.63	7.41	62.12	61.84	96.695	[5]
Flaxseed	Three-necked flat bottom flask, magnetic stirrer	KOH	0.4–1.0	Methanol	4:1–6:1	30–60	35–65	Absent	RSM, FCCD	0.51	5.9	33	59	98 ± 2	[57]
Carica papaya	Three-neck laboratory reactors, magnetic stirrer	KOH	0.5–1.5	Methanol	4:1–10:1	60	45–65	600	RSM, Box-Behnken	1.0	10	60	45	96.48	[47]
Ailanthus altissima seed	Ultrasonication device, amplitude: 70%, pulse: 70	KOH	1–2	Methanol	2:1–12:1	2–10	50	Absent	RSM, Box-Behnken	1.01	8.5:1	4.71	50	92.26	[81]

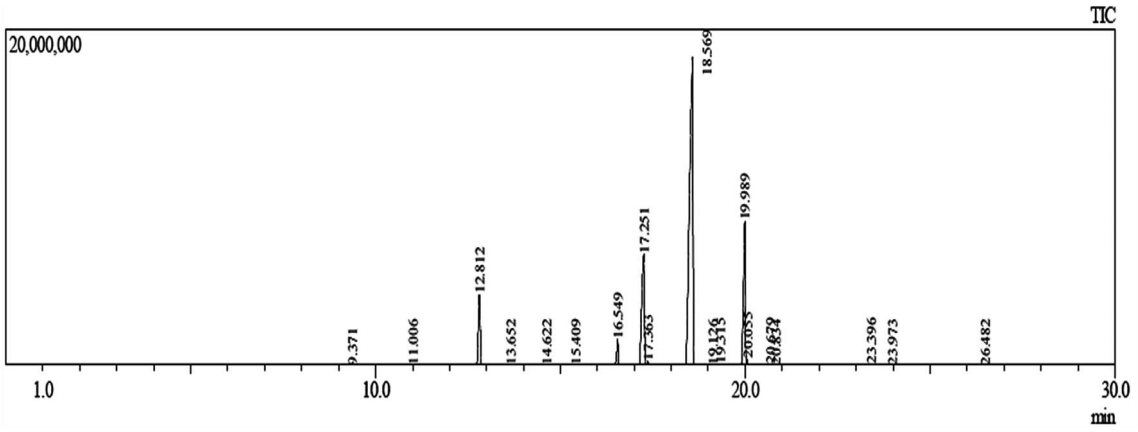

Figure 10. Chromatograph outcomes for HSOB.

Table 6. Comparison of fatty acid profiles of *Cannabis sativa* L. seed oil biodiesel and other biodiesels produced with different feedstocks.

Fatty acid		Structure	Formula	Molecular mass kg/kmol	Current study (%)	Kusum [68]	*Cannabis sativa* L. [84]	*Styrax officinalis* L. [76]	Sunflower [85]	Pearl millet [86]
Common name	Systematic name									
Myristic	Tetradecanoic	14:0	$C_{14}H_{28}O_2$	228	0.04	–	–	0.03	–	–
Pentadecanoic	Pentadecanoic	15:0	$C_{15}H_{30}O_2$	242	0.02	–	–	–	–	–
Palmitic	Hexadecanoic	16:0	$C_{16}H_{32}O_2$	256	7.01	9.89	6.52	8.08	7.29	21.90
Palmitoleic	Hexadec-9-enoic	16:1	$C_{16}H_{30}O_2$	254	0.12	–	0.07	0.01	–	0.10
Margaric	Heptadecanoic	17:0	$C_{17}H_{34}O_2$	270	0.07	–	–	0.10	–	–
Margaroleic	Cis-9-Heptadecenoic	17:1	$C_{17}H_{32}O_2$	268	0.04	–	–	0.14	–	–
Stearic	Octadecanoic	18:0	$C_{18}H_{36}O_2$	284	3.22	3.63	2.81	3.00	13.55	3.40
Oleic	Cis-9-Octadecanoic	18:1	$C_{18}H_{34}O_2$	282	15.65	44.2	15.25	23.22	18.79	–
Elaidic	Octadec-9-enoic	18:1	$C_{18}H_{34}O_2$	282	0.77	–	0.75	–	–	–
Linoleic	Cis-9-cis-12 Octadecanoic	18:2	$C_{18}H_{32}O_2$	280	54.27	1.8	55.44	64.41	58.98	73.90
Linolelaidic	Octadeca-9,12-dienoic	18:2	$C_{18}H_{32}O_2$	280	0.15	–	0.34	–	–	–
Gamma-Linolenic	Cis-6,9,12 Octadecatrienoic	18:3	$C_{18}H_{30}O_2$	278	0.37	–	–	–	–	–
Alpha-Linolenic	Cis-9-cis-12 Octadecatrienoic	18:3	$C_{18}H_{30}O_2$	278	16.51	–	17.91	0.10	0.12	–
Stearidonic	Octadeca-6,9,12,15-tetraenoic	18:4	$C_{18}H_{28}O_2$	276	0.17	–	–	–	–	–
Arachidic	Eicosanoic	20:0	$C_{20}H_{40}O_2$	312	0.73	15.27	0.36	0.07	0.33	0.30
Gondoic	Cis-11-Eicosenoic	20:1	$C_{20}H_{38}O_2$	310	0.41	18.19	0.15	0.12	–	0.30
Behenic	Docosanoic	22:0	$C_{22}H_{44}O_2$	341	0.35	3.82	0.23	0.47	0.93	–
Erucic	Cis-13-Docosenoic	22:1	$C_{22}H_{42}O_2$	338	0.02	–	0.07	0.25	–	–
Lignoceric	Tetracosanoic	24:0	$C_{24}H_{48}O_2$	368	0.12	–	0.09	–	–	0.10
Other	–	–	–	–	–	3.2	–	–	–	–
Saturated fatty acids					11.44	32.61	10.01	11.75	22.10	25.70
Monounsaturated fatty acids					17.13	–	16.30	23.74	18.79	0.40
Polyunsaturated fatty acids					71.47	–	73.69	64.51	59.10	73.90
Unsaturated fatty acids					88.60	64.19	89.99	88.25	77.89	74.30
Total fatty acids					100.00	100.00	100.00	100.00	99.99	100.00
DU					160.07	–	163.68	152.86	136.99	148.20
LCSF					3.81	–	2.942	7.67	–	–

Table 7. Comparison of physical and chemical properties of biodiesel produced from *Cannabis sativa* L. and other raw materials based on the EN 14214 standard.

No	Property	Unit	EN 14214		This study	Sterculia foetida [79]	Sinapis alba [5]	Grape seed oil biodiesel [87]	Flaxseed oil biodiesel [57]
			Min.	Max.					
1	Higher heating value	kJ/kg	–	–	38.80	39.86	39.931	39.95	40.46
2	Density at 15 °C	g/cm^3	0.86	0.90	0.872	0.892	0.878	0.882	0.876
3	Kinematic viscosity at 40 °C	mm^2/s	3.50	5.00	4.329	5.579	5.413	4.32	2.97
4	Cetane number	–	51	–	37.36	–	57.23	52.8	43
5	Acid value	mg KOH/g	–	0.50	0.40	–	0.336	–	2.24
6	Iodine value	g iodine/100 g	–	120	160.66	90.4	106.26	–	169.11
7	Oxidation stability	min	–	8	9.42	–	–	–	–
8	Saponification number	mg KOH/g	–	–	200.63	–	–	–	157.08
9	Linolenic acid methyl ester	(m/m)%	–	–	0	–	11.701	–	–
10	Polyunsaturated methyl ester (≥4 double bonds)	(m/m)%	–	1.0	0.17	–	0	–	–
11	Color	–	–	–	Dark greenish	–	2.0	–	Yellow orange
12	Physical state at room temperature	–	–	–	Liquid	–	–	–	–
13	Flash point	°C	101	–	>120	162	164	–	171
14	Cloud point	°C	Report		−1.30	1	5	−6.2	−4
15	Cold filter plugging point	°C	Report		−4.52	–	0	−10.5	–
16	Pour point	°C	–	–	−6.87	−3	−18	−8	−9
17	Carbon	wt.%	77		77.11	77.34	–	76.90	–
18	Hydrogen	wt.%	12		11.16	11.90	–	11.30	–
19	Oxygen	wt.%	11		11.73	10.27	–	–	–
20	Copper strip corrosion, 3 h at 50 °C	Degree of corrosion	Class 1		1a	–	1a	–	–
21	P content	mg/kg	–	1.0	–	4.1	9.254	–	–
22	Mn content	mg/kg	–	–	0.093	–	–	–	–
23	Group I metals (Na + K)	mg/kg	–	5.0	136.59	–	56.15	–	–
24	Group II metals (Ca + Mg)	mg/kg	–	5.0	4.95	–	25.117	–	–

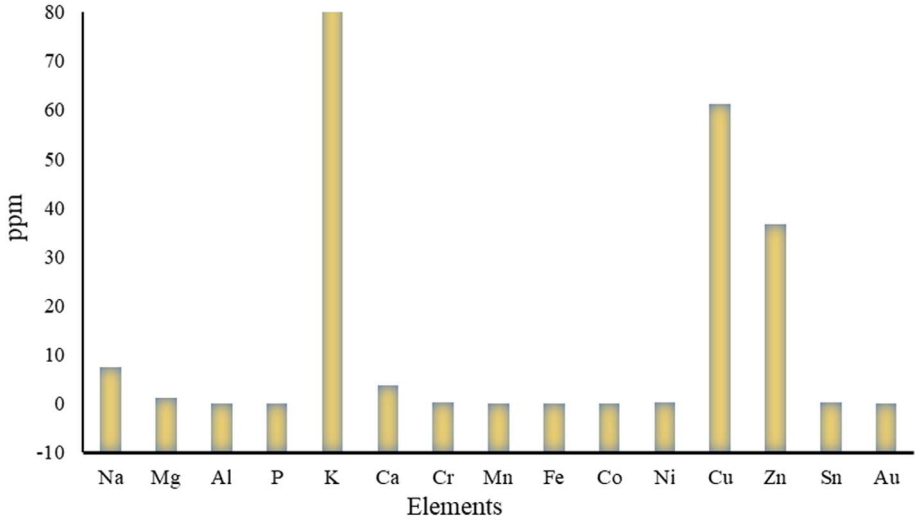

Figure 11. Fundamental elemental analysis of biodiesel produced from *Cannabis sativa* L. seed oil.

Compared to all other examples in Table 7, including this study, the higher heating values showed a significant degree of similarity. The results indicated that the majority of the physical and chemical characteristics of *Cannabis sativa* L. seed oil biodiesel met the set norms. This suggests that it can be used in diesel engines instead of diesel fuel made from petroleum.

Figure 11 illustrates the findings of the elemental analysis conducted on the biodiesel derived from *Cannabis sativa* L. seed oil. The biodiesel sample does not contain detectable

levels of Al, P, Fe, or Co. However, it was determined that the Cr, Mn, Ni, Sn, and Cu contents were below 1 ppm. The element with the highest abundance was potassium (K), which had a concentration of 129.24 parts per million (ppm), followed by copper (Cu) and zinc (Zn), with concentrations of 61.17 ppm and 36.54 ppm, respectively.

4 Conclusions and future directions

The current experimental research is a comprehensive study that performs the statistical optimization of critical process parameters such as methanol to oil molar ratio (increased by 2:1 each from 2:1 to 10:1), catalyst concentration (increased by 0.2 wt.% each from 0.4 wt.% to 1.2 wt.%), reaction temperature (increased by 15 °C each from 50 °C to 70 °C), and reaction time (increased by 20 min each from 20 min to 100 min) with the RSM to achieve the highest efficiency in biodiesel production using the oil of *Cannabis sativa* L. seeds. The five-level, four-factor CCD design was used to establish the experimental strategy and optimization matrix to optimize the conversion process of HSOB. According to EN 14214 specifications, the HSOB's physicochemical characteristics were assessed and compared to those of other biodiesels. Based on the obtained data, it is possible to derive the following conclusions:

- The RSM projected that the alkaline-catalyzed transesterification process would have an optimal methanol-to-oil molar ratio of 7.4141:1, a catalyst concentration of 0.8040 wt.%, a reaction temperature of 61.9192 °C, and a reaction time of 62.8283 min.
- The HSOB yield in the experiment study, which involved three replicates and the aforementioned conditions, was 95.24%, which is close to the maximum HSOB yield RSM predicted (96.14%) for the same optimum values of the process variables.
- The calculated R^2 value of 0.9614 suggests that the RSM accounts for 96.14% of the observed variability in the yield of HSOB. The R^2 value demonstrates the reliability of the RSM in predicting the optimal variables for the alkaline-catalyzed transesterification process.
- Based on the ANOVA findings, it was determined that the methanol-to-oil molar ratio exhibited the highest level of significance compared to the other parameters that were investigated.
- The fuel characteristics of hemp seed oil biodiesel follow close values to studies on biodiesel produced from other oilseeds. It also meets the EN 14214 standard, except for a few, such as iodine value, Group I metals, etc.

The use of GC-MS analysis and subsequent characterization has substantiated the enhanced quality of biodiesel, thereby establishing its suitability for future implementation in the automotive industry. This study also yields significant findings about the development of efficient and sustainable processes for producing biodiesel from non-edible oils within a contemporary framework. This investigation's findings indicate there is no threat to safety. A carefully chosen corrective strategy should be implemented to produce non-edible-based biodiesel more economically viable on an industrial level. In order to mitigate the potential inflationary effects on food prices, it is essential to subject the trade of biodiesel derived from edible resources to rigorous governmental oversight.

For future studies, it would be interesting to investigate the use of other non-edible oils as feedstocks for biodiesel production, such as jatropha oil or algal oil. Additionally, further research could be conducted to optimize the process conditions for the production of biodiesel from hemp seed oil, such as exploring different catalysts or reaction conditions. Moreover, a techno-economic analysis and life cycle assessment of the biodiesel production process from hemp seed oil could provide valuable insights into the feasibility and sustainability of this technology. Finally, investigating the potential use of hemp seed oil biodiesel in different applications, such as aviation or marine fuels, could help to expand the market for this sustainable fuel source.

Acknowledgements

The authors would like to thank the editors and anonymous reviewers for helping us to present a balanced account of our paper. The authors sincerely thank The Scientific and Technological Research Council of Turkey (TUBITAK).

Funding

The present study has been supported by The Scientific and Technological Research Council of Turkey (TUBITAK) during the 2209-A-2021/2 period (University Students Domestic Research Projects Support Program) working on projects numbered 1919B012105287.

Conflict of interest

The authors pointed out that there is no potential conflict of interest.

Data availability

The data used and/or analyzed throughout the present study are available from the authors upon reasonable request. The authors declared that there is no competing financial interest in this research.

Authors' contributions

Cemal Yazilitas and Zeki Yilbasi: Conceptualization, Investigation, Methodology, Formal analysis, Visualization, Data curation, Validation, Resources, Writing – original draft, Writing – review & editing. Murat Kadir Yesilyurt: Methodology, Data curation, Validation, Formal analysis, Visualization, Writing – original draft, Writing – review & editing.

Ethical approval

The authors declared that no animal and human studies are presented in this manuscript and no potentially identifiable human images or data are given in this research.

References

1 IEA (2021) Energy access outlook 2021: From poverty to prosperity. Available at https://www.iea.org/reports/energy-access-outlook-2021.

2 UNDP (2021) Sustainable development goal 7: affordable and clean energy. Available at https://www.undp.org/sustainable-development-goals/affordable-and-clean-energy.
3 World Bank (2021) Energy access. Available at https://www.worldbank.org/en/topic/energyaccess.
4 United Nations (2021) Sustainable development goals report 2021. Available at https://unstats.un.org/sdgs/report/2021/.
5 Yesilyurt M.K., Arslan M., Eryilmaz T. (2019) Application of response surface methodology for the optimization of biodiesel production from yellow mustard (*Sinapis alba* L.) seed oil, *Int. J. Green Energy* **16**, 1, 60–71. https://doi.org/10.1080/15435075.2018.1532431.
6 Zakeri B., Paulavets K., Barreto-Gomez L., Echeverri L.G., Pachauri S., Boza-Kiss B., Pouya S. (2022) Pandemic, war, and global energy transitions, *Energies* **15**, 17, 6114. https://doi.org/10.3390/en15176114.
7 Arora N.K., Mishra I. (2022) Current scenario and future directions for sustainable development goal 2: A roadmap to zero hunger, *Environ. Sustain.* **5**, 2, 129–133.
8 Hienuki S., Mitoma H., Ogata M., Uchida I., Kagawa S. (2021) Environmental and energy life cycle analyses of passenger vehicle systems using fossil fuel-derived hydrogen, *Int. J. Hydrogen Energy* **46**, 73, 36569–36580. https://doi.org/10.1016/j.ijhydene.2021.08.135.
9 Holechek J.L., Geli H.M., Sawalhah M.N., Valdez R. (2022) A global assessment: can renewable energy replace fossil fuels by 2050? *Sustainability* **14**, 8, 4792. https://doi.org/10.3390/su14084792.
10 Ajanovic A., Haas R. (2021) Prospects and impediments for hydrogen and fuel cell vehicles in the transport sector, *Int. J. Hydrogen Energy* **46**, 16, 10049–10058. https://doi.org/10.1016/j.ijhydene.2020.03.122.
11 Kober T., Schiffer H.W., Densing M., Panos E. (2020) Global energy perspectives to 2060–WEC's World Energy Scenarios 2019, *Energy Strategy Rev.* **31**, 100523. https://doi.org/10.1016/j.esr.2020.100523.
12 Harrington A., Hall J., Bassett M., Lu E., Zhao H. (2022) *Combustion Characteristics and Exhaust Emissions of a Direct Injection SI Engine with Pure Ethanol and Methanol in Comparison to Gasoline (No. 2022-01-1089)*. SAE Technical Paper. https://doi.org/10.4271/2022-01-1089.
13 Salamai A.A., Faisal S.M., Khan A.K. (2022) The relationship between inflation and GDP with reference to oil based economy, *Int. J. Multidiscip. Res. Growth Eval.*. Available at: https://www.allmultidisciplinaryjournal.com/uploads/archives/620B85264EDD61644922150.pdf.
14 Li H., Liu Y., Luo X., Duan H. (2022) A novel nonlinear multivariable Verhulst grey prediction model: A case study of oil consumption forecasting in China, *Energy Rep.* **8**, 3424–3436. https://doi.org/10.1016/j.egyr.2022.02.149.
15 Fayyazbakhsh A., Bell M.L., Zhu X., Mei X., Koutný M., Hajinajaf N., Zhang Y. (2022) Engine emissions with air pollutants and greenhouse gases and their control technologies, *J. Clean. Prod.* 134260. https://doi.org/10.1016/j.jclepro.2022.134260.
16 Masera K., Hossain A.K. (2023) Advancement of biodiesel fuel quality and NOx emission control techniques. *Renew. Sustain. Energy Rev.* **178**, 113235. https://doi.org/10.1016/j.rser.2023.113235.
17 Gielen D., Boshell F., Saygin D., Bazilian M.D., Wagner N., Gorini R. (2019) The role of renewable energy in the global energy transformation, *Energy Strategy Rev.* **24**, 38–50. https://doi.org/10.1016/j.esr.2019.01.006.
18 Ali A., Mushtaq A. (2023) Do biofuels really a need of the day: Approaches, mechanisms, applications and challenges, *Int. J. Chem. Biochem. Sci.* **23**, 219–226. Available at: https://www.iscientific.org/wp-content/uploads/2023/05/25-IJCBS-23-23-28.pdf.
19 Zhang S., Huang W., Huang Y.A., Zhang C. (2020) Plant species recognition methods using leaf image: Overview, *Neurocomputing* **408**, 246–272. https://doi.org/10.1016/j.neucom.2019.09.113.
20 Basoglu F. (2018) *Yemeklik yağ teknolojisi*, 6th ed., Dora Publishing, Bursa, Turkey, p. 385.
21 Lafarga T. (2021) Production and consumption of oils and oilseeds, in: *Oil and Oilseed Processing: Opportunities and Challenges*, pp. 1–21. https://doi.org/10.1002/9781119575313.ch1.
22 Kepekci H. (2019) Bioenergy potential for energy generation from agriculture in Turkey, *Eur. Int. J. Sci. Technol.* **8**, 3, 1–14. https://eijst.org.uk/articles/8.3.1.1-14.pdf.
23 Ragit S.S., Mohapatra S.K., Gill P., Kundu K. (2012) Brown hemp methyl ester: transesterification process and evaluation of fuel properties, *Biomass Bioenergy* **41**, 14–20. https://doi.org/10.1016/j.biombioe.2011.12.026.
24 Rehman M.S.U., Rashid N., Saif A., Mahmood T., Han J.I. (2013) Potential of bioenergy production from industrial hemp (Cannabis sativa): Pakistan perspective, *Renew. Sustain. Energy Rev.* **18**, 154–164. https://doi.org/10.1016/j.rser.2012.10.019.
25 John C.B., Raja S.A. (2020) Analysis of combustion, emission and performance attributes of hemp biodiesel on a compression ignition engine, *World Rev. Sci. Technol. Sustain. Dev.* **16**, 2, 169–183. https://doi.org/10.1504/WRSTSD.2020.109724.
26 Naeem M.Y., Corbo F., Crupi P., Clodoveo M.L. (2023) Hemp: An alternative source for various industries and an emerging tool for functional food and pharmaceutical sectors, *Processes* **11**, 3, 718. https://doi.org/10.3390/pr11030718.
27 Ely K., Podder S., Reiss M., Fike J. (2022) Cannabis/hemp: Sustainable uses, opportunities, and current limitations, in *Cannabis/Hemp for Sustainable Agriculture and Materials*, pp. 59–87. https://link.springer.com/chapter/10.1007/978-981-16-8778-5_3.
28 Tripathi A., Kumar R. (2022) Industrial hemp for sustainable agriculture: A critical evaluation from global and Indian perspectives, in *Cannabis/Hemp for Sustainable Agriculture and Materials*, Springer Singapore, Singapore, pp. 29–57.
29 Ahmad M., Ullah K., Khan M.A., Zafar M., Tariq M., Ali S., Sultana S. (2011) Physicochemical analysis of hemp oil biodiesel: A promising non edible new source for bioenergy, *Energy Sources A: Recovery Util. Environ. Eff.* **33**, 14, 1365–1374. https://doi.org/10.1080/15567036.2010.499420.
30 Yilbaşi Z., Yesilyurt M.K., Yaman H., Arslan M. (2022) The industrial-grade hemp (*Cannabis sativa* L.) seed oil biodiesel application in a diesel engine: combustion, harmful pollutants, and performance characteristics, *Sci. Technol. Energy Transit.* **77**, 15. https://doi.org/10.2516/stet/2022011.
31 Capuano D., Costa M., Di Fraia S., Massarotti N., Vanoli L. (2017) Direct use of waste vegetable oil in internal combustion engines, *Renew. Sustain. Energy Rev.* **69**, 759–770. https://doi.org/10.1016/j.rser.2016.11.016.
32 Sonthalia A., Kumar N. (2019) Hydroprocessed vegetable oil as a fuel for transportation sector: A review, *J. Energy Inst.* **92**, 1, 1–17. https://doi.org/10.1016/j.joei.2017.10.008.
33 Yaşar F. (2020) Comparision of fuel properties of biodiesel fuels produced from different oils to determine the most suitable feedstock type, *Fuel* **264**, 116817. https://doi.org/10.1016/j.fuel.2019.116817.
34 Kharia P., Saini R., Kudapa V.K. (2023) A study on various sources and technologies for production of biodiesel and its efficiency, *MRS Energy Sustain.* **10**, 1, 35–51. https://link.springer.com/article/10.1557/s43581-022-00058-4.
35 Encinar J.M., Nogales S., González J.F. (2020) Biodiesel and biolubricant production from different vegetable oils through transesterification, *Eng. Rep.* **2**, 12, e12190. https://doi.org/10.1002/eng2.12190.
36 Mishra V.K., Goswami R. (2018) A review of production, properties and advantages of biodiesel, *Biofuels* **9**, 2, 273–289. https://doi.org/10.1080/17597269.2017.1336350.
37 Hanif M.A., Nisar S., Akhtar M.N., Nisar N., Rashid N. (2018) Optimized production and advanced assessment of biodiesel: A review, *Int. J. Energy Res.* **42**, 6, 2070–2083. https://doi.org/10.1002/er.3990.
38 Suraj C.K., Anand K., Sundararajan T. (2020) Investigation of biodiesel production methods by altering free fatty acid content in vegetable oils, *Biofuels* **11**, 5, 587–595. https://doi.org/10.1080/17597269.2017.1378993.
39 Mandari V., Devarai S.K. (2021) Biodiesel production using homogeneous, heterogeneous, and enzyme catalysts via transesterification and esterification reactions: A critical review, *BioEnergy Res.* **15**, 1–27. https://link.springer.com/article/10.1007/s12155-021-10333-w.

40 Babadi A.A., Rahmati S., Fakhlaei R., Barati B., Wang S., Doherty W., Ostrikov K.K. (2022) Emerging technologies for biodiesel production: Processes, challenges, and opportunities, *Biomass Bioenergy* **163**, 106521. https://doi.org/10.1016/j.biombioe.2022.106521.

41 Jahirul M.I., Koh W., Brown R.J., Senadeera W., O'Hara I., Moghaddam L. (2014) Biodiesel production from non-edible beauty leaf (*Calophyllum inophyllum*) oil: Process optimization using response surface methodology (RSM), *Energies* **7**, 8, 5317–5331. https://doi.org/10.3390/en7085317.

42 Ahmed Elgharbawy A. (2021) Transesterification reaction conditions and low-quality feedstock treatment processes for biodiesel production – A review, *J. Petrol. Mining Eng.* **23**, 1, 89–94. https://dx.doi.org/10.21608/jpme.2021.67482.1076.

43 Soosai M.R., Moorthy I.M.G., Varalakshmi P., Yonas C.J. (2022) Integrated global optimization and process modelling for biodiesel production from non-edible silk-cotton seed oil by microwave-assisted transesterification with heterogeneous calcium oxide catalyst, *J. Clean. Prod.* **367**, 132946. https://doi.org/10.1016/j.jclepro.2022.132946.

44 Xie W., Wan F. (2019) Immobilization of polyoxometalate-based sulfonated ionic liquids on UiO-66-2COOH metal-organic frameworks for biodiesel production via one-pot transesterification-esterification of acidic vegetable oils, *Chem. Eng. J.* **365**, 40–50. https://doi.org/10.1016/j.cej.2019.02.016.

45 Aleman-Ramirez J.L., Okoye P.U., Torres-Arellano S., Paraguay-Delgado F., Mejía-López M., Moreira J., Sebastian P.J. (2022) Development of reusable composite eggshell-moringa leaf catalyst for biodiesel production, *Fuel* **324**, 124601. https://doi.org/10.1016/j.fuel.2022.124601.

46 Gupta A.R., Jalan A.P., Rathod V.K. (2018) Solar energy as a process intensification tool for the biodiesel production from hempseed oil, *Energy Conv. Manag.* **171**, 126–132. https://doi.org/10.1016/j.enconman.2018.05.050.

47 Anwar M., Rasul M.G., Ashwath N. (2018) Production optimization and quality assessment of papaya (*Carica papaya*) biodiesel with response surface methodology, *Energy Convers. Manag.* **156**, 103–112. https://doi.org/10.1016/j.enconman.2017.11.004.

48 Islam M.S., Hart C.R., Casadonte D. (2022) Ultrasound-assisted solid Lewis acid-catalyzed transesterification of *Lesquerella fendleri* oil for biodiesel synthesis, *Ultrason. Sonochem.* **88**, 106082. https://doi.org/10.1016/j.ultsonch.2022.106082.

49 Khan Z., Javed F., Shamair Z., Hafeez A., Fazal T., Aslam A., Zimmerman W.B., Rehman F. (2021) Current developments in esterification reaction: A review on process and parameters, *J. Ind. Eng. Chem.* **103**, 80–101. https://doi.org/10.1016/j.jiec.2021.07.018.

50 Mulyatun M., Prameswari J., Istadi I., Widayat W. (2022) Production of non-food feedstock based biodiesel using acid-base bifunctional heterogeneous catalysts: A review, *Fuel* **314**, 122749. https://doi.org/10.1016/j.fuel.2021.122749.

51 Singh N.K., Singh Y., Sharma A. (2022) Optimization of biodiesel synthesis from Jojoba oil via supercritical methanol: A response surface methodology approach coupled with genetic algorithm, *Biomass Bioenergy* **156**, 106332. https://doi.org/10.1016/j.biombioe.2021.106332.

52 Tarigan J.B., Singh K., Sinuraya J.S., Supeno M., Sembiring H., Tarigan K., Sitepu E.K. (2022) Waste passion fruit peel as a heterogeneous catalyst for room-temperature biodiesel production, *ACS Omega* **7**, 9, 7885–7892. https://doi.org/10.1021/acsomega.1c06785.

53 Yesilyurt M.K., Cesur C. (2022) A statistical optimization attempt by applying the Taguchi technique for the optimum transesterification process parameters in the production of biodiesel from *Papaver somniferum* L. seed oil, *Fuel* **329**, 125406. https://doi.org/10.1016/j.fuel.2022.125406.

54 Elgharbawy A.S., Sadik W., Sadek O.M., Kasaby M.A. (2021) A review on biodiesel feedstocks and production technologies, *J. Chil. Chem. Soc.* **66**, 1, 5098–5109. https://doi.org/10.4067/S0717-97072021000105098.

55 Dagdelen A., Yuksel Y. (2016) The effects of oilseed variety and transesterification method on biofuel production and quality, *Nevsehir J. Sci. Technol. Spec. Issue* 107–17. https://doi.org/10.17100/nevbiltek.210972.

56 Dharma S.M.H.H., Masjuki H.H., Ong H.C., Sebayang A.H., Silitonga A.S., Kusumo F., Mahlia T.M.I. (2016) Optimization of biodiesel production process for mixed *Jatropha curcas* – Ceiba pentandra biodiesel using response surface methodology, *Energy Convers. Manag.* **115**, 178–190. https://doi.org/10.1016/j.enconman.2016.02.034.

57 Ahmad T., Danish M., Kale P., Geremew B., Adeloju S.B., Nizami M., Ayoub M. (2019) Optimization of process variables for biodiesel production by transesterification of flaxseed oil and produced biodiesel characterizations, *Renew. Energy* **139**, 1272–1280. https://doi.org/10.1016/j.renene.2019.03.036.

58 Marwaha A., Rosha P., Mohapatra S.K., Mahla S.K., Dhir A. (2019) Biodiesel production from Terminalia bellerica using eggshell-based green catalyst: An optimization study with response surface methodology, *Energy Rep.* **5**, 1580–1588. https://doi.org/10.1016/j.egyr.2019.10.022.

59 Danish M., Ahmad T., Ayoub M., Geremew B., Adeloju S. (2020) Conversion of flaxseed oil into biodiesel using KOH catalyst: Optimization and characterization dataset, *Data Br.* **29**, 105225. https://doi.org/10.1016/j.dib.2020.105225.

60 Qu T., Niu S., Zhang X., Han K., Lu C. (2021) Preparation of calcium modified Zn-Ce/Al_2O_3 heterogeneous catalyst for biodiesel production through transesterification of palm oil with methanol optimized by response surface methodology, *Fuel* **284**, 118986. https://doi.org/10.1016/j.fuel.2020.118986.

61 Almasi S., Najafi G., Ghobadian B., Jalili S. (2021) Biodiesel production from sour cherry kernel oil as novel feedstock using potassium hydroxide catalyst: Optimization using response surface methodology, *Biocatal. Agric. Biotechnol.* **35**, 102089. https://doi.org/10.1016/j.bcab.2021.102089.

62 Karimi S., Saidi M. (2022) Biodiesel production from Azadirachta India-derived oil by electrolysis technique: Process optimization using response surface methodology (RSM), *Fuel Process. Technol.* **234**, 107337. https://doi.org/10.1016/j.fuproc.2022.107337.

63 Kumar S., Deswal V. (2022) Optimization at low temperature transesterification biodiesel production from soybean oil methanolysis via response surface methodology, *Energy Sources A: Recovery Util. Environ. Eff.* **44**, 1, 2284–2293. https://doi.org/10.1080/15567036.2019.1649331.

64 Kumar S. (2023) Application of response surface methodology for the optimisation of biodiesel production from Jatropha-algae oil blend, *Int. J. Ambient Energy* **44**, 1, 1557–1562. https://doi.org/10.1080/01430750.2023.2179109.

65 Prodhan A., Hasan M.I., Sujan S.M.A., Hossain M., Quaiyyum M.A., Ismail M. (2020) Production and characterization of biodiesel from Jatropha (*Jatropha curcas*) seed oil available in Bangladesh, *Energy Sources A: Recovery Util. Environ. Eff.* 1–16. https://doi.org/10.1080/15567036.2020.1851819.

66 Suzihaque M.U.H., Syazwina N., Alwi H., Ibrahim U.K., Abdullah S., Haron N. (2022) A sustainability study of the processing of kitchen waste as a potential source of biofuel: Biodiesel production from waste cooking oil (WCO), *Mater. Today Proc.* **63**, S484–S489. https://doi.org/10.1016/j.matpr.2022.04.526.

67 Özgür C. (2021) Optimization of biodiesel yield and diesel engine performance from waste cooking oil by response surface method (RSM), *Petrol. Sci. Technol.* **39**, 17–18, 683–703. https://doi.org/10.1080/10916466.2021.1954019.

68 Pali H.S., Sharma A., Kumar N., Singh Y. (2021) Biodiesel yield and properties optimization from Kusum oil by RSM, *Fuel* **291**, 120218. https://doi.org/10.1016/j.fuel.2021.120218.

69 Bai M.T., Swarna U., Raju C.A., Sridevi V. (2021) Production of methyl ester from mahua oil: Characterization and optimization by using RSM, *Mater. Today Proc.* **44**, 1609–1616. https://doi.org/10.1016/j.matpr.2020.11.815.

70 Hashemzehi M., Pirouzfar V., Nayebzadeh H., Su C.H. (2022) Modelling and optimization of main independent parameters for biodiesel production over a $Cu_{0.4}Zn_{0.6}Al_2O_4$ catalyst using an RSM method, *J. Chem. Technol. Biotechnol.* **97**, 1, 111–119. https://doi.org/10.1002/jctb.6916.

71 Karimi K., Saidi M., Moradi P., Taheri Najafabadi A. (2023) Biodiesel production from *Nannochloropsis* microalgal biomass-derived oil: An experimental and theoretical study using the RSM-CCD approach, *Can. J. Chem. Eng.* https://doi.org/10.1002/cjce.24863.

72 Pali H.S., Sharma A., Kumar M., Annakodi V.A., Singh N.K., Singh Y., Nguyen P.Q.P. (2023) Enhancement of combustion characteristics of waste cooking oil biodiesel using TiO_2 nanofluid blends through RSM, *Fuel* **331**, 125681. https://doi.org/10.1016/j.fuel.2022.125681.

73 Manojkumar N., Muthukumaran C., Sharmila G. (2022) A comprehensive review on the application of response surface methodology for optimization of biodiesel production using different oil sources, *J. King Saud Univ. Eng. Sci.* **34**, 3, 198–208. https://doi.org/10.1016/j.jksues.2020.09.012.

74 Kokkinos N., Lazaridou A., Stamatis N., Orfanidis S., Mitropoulos A. C., Christoforidis A., Nikolaou N. (2015) Biodiesel production from selected microalgae strains and determination of its properties and combustion specific characteristics, *J. Eng. Sci. Technol. Rev.* **8**, 4, 1–6. https://pdfs.semanticscholar.org/b44b/15dad6a98d24b82f70b95e5ed2757cf1e8f0.pdf.

75 Abdulvahitoğlu A. (2019) Predicted fuel characteristics of prunus avium seed oil as a candidate for biodiesel production, *Int. J. Automot. Eng. Technol.* **8**, 4, 165–171. https://doi.org/10.18245/ijaet.625754.

76 Yesilyurt M.K., Cesur C. (2020) Biodiesel synthesis from *Styrax officinalis* L. seed oil as a novel and potential non-edible feedstock: A parametric optimization study through the Taguchi technique, *Fuel* **265**, 117025. https://doi.org/10.1016/j.fuel.2020.117025.

77 Mofijur M., Ahmed S.F., Rony Z.I., Khoo K.S., Chowdhury A.A., Kalam M.A., Khan T.Y. (2023) Screening of non-edible (second-generation) feedstocks for the production of sustainable aviation fuel, *Fuel* **331**, 125879. https://doi.org/10.1016/j.fuel.2022.125879.

78 Venkatesan H., Sivamani S. (2022) Evaluating the predicting capability of response surface methodology on biodiesel production from grape seed bio-oil, *Energy Sources A: Recovery Util. Environ. Eff.* **44**, 1, 2473–2488. https://doi.org/10.1080/15567036.2019.1649759.

79 Marri V.B., Kotha M.M., Gaddale A.P.R. (2022) Production process optimisation of *Sterculia foetida* methyl esters (biodiesel) using response surface methodology, *Int. J. Ambient Energy* **43**, 1, 1837–1846. https://doi.org/10.1080/01430750.2020.1723692.

80 Kumar P., Kumar N. (2021) Process optimization for production of biodiesel from orange peel oil using response surface methodology, *Energy Sources A: Recovery Util. Environ. Eff.* **43**, 6, 727–737. https://doi.org/10.1080/15567036.2019.1631909.

81 Hoseini S.S., Najafi G., Ghobadian B., Mamat R., Ebadi M.T., Yusaf T. (2018) Ailanthus altissima (tree of heaven) seed oil: Characterisation and optimisation of ultrasonication-assisted biodiesel production, *Fuel* **220**, 621–630. https://doi.org/10.1016/j.fuel.2018.01.094.

82 Bhuiya M.M.K., Rasul M.G., Khan M.M.K., Ashwath N. (2020) Biodiesel production and characterisation of poppy (*Papaver somniferum* L.) seed oil methyl ester as a source of 2nd generation biodiesel feedstock, *Ind. Crops Prod.* **152**, 112493. https://doi.org/10.1016/j.indcrop.2020.112493.

83 Saravanan A., Kings A.J., Miriam L.M., Isaac R.R. (2022) RSM-based comparative experimental study of sustainable biodiesel synthesis from different 2G feedstocks using magnetic nanocatalyst $CaFe_2O_4$, *Environ. Dev. Sustain.* **26**, 2, 1–30. https://link.springer.com/article/10.1007/s10668-022-02761-1.

84 Yilbaşi Z., Yesilyurt M.K., Arslan M. (2023) The production of methyl ester from industrial grade hemp (*Cannabis sativa* L.) seed oil: a perspective of Turkey – the optimization study using the Taguchi method, *Biomass Convers. Biorefin.* **13**, 11, 9955–9975. https://link.springer.com/article/10.1007/s13399-021-01751-z.

85 Niyas M.M., Shaija A. (2022) Effect of repeated heating of coconut, sunflower, and palm oils on their fatty acid profiles, biodiesel properties and performance, combustion, and emission, characteristics of a diesel engine fueled with their biodiesel blends, *Fuel* **328**, 125242. https://doi.org/10.1016/j.fuel.2022.125242.

86 Perveen S., Hanif M.A., Nadeem R., Rashid U., Azeem M.W., Zubair M., Moser B.R. (2021) A novel route of mixed catalysis for production of fatty acid methyl esters from potential seed oil sources, *Catalysts* **11**, 7, 811. https://doi.org/10.3390/catal11070811.

87 Bolonio D., García-Martínez M.J., Ortega M.F., Lapuerta M., Rodríguez-Fernández J., Canoira L. (2019) Fatty acid ethyl esters (FAEEs) obtained from grapeseed oil: A fully renewable biofuel, *Renew. Energy* **132**, 278–283. https://doi.org/10.1016/j.renene.2018.08.010.